were kept to a minimum by the data-taking sequence and the number of individual measurements made of μ. An indication of the size of these errors is given by the standard deviations in Table I. Since the sample impurity corrections are small, the errors in this correction are believed to be quite small. The only possible exception to this is the Be data where the impurity correction varies from zero to twelve percent. Errors in the Be attenuation coefficients are believed to be less than 2%. There are no known sources of systematic errors in the present work.

ACKNOWLEDGMENTS

The authors express their appreciation for the many helpful discussions with Prof. G. B. Arfken, Miami University, Oxford, Ohio. They also acknowledge the assistance of J. R. Brown who wrote the computer program used in analyzing the data.

PHYSICAL REVIEW VOLUME 153, NUMBER 2 10 JANUARY 1967

Relaxation of OH^- Dipoles in KCl at Low Temperatures*

LAWRENCE A. VREDEVOE†
University of California, Los Angeles, California
(Received 11 April 1966; revised manuscript received 23 June 1966)

The direct and Raman relaxation rates of OH^- electric dipoles in KCl are computed using a point-charge–point-dipole model in which we allow for the possibility that the equilibrium position of the dipole is displaced from the center of octahedral symmetry. This model can thus include the effect of an OH^- quadrupole moment. Such a moment can be represented by an effective displacement of the dipole. Estimates are made of the rates at temperatures between 2 and 11°K in the presence of weak and strong dc electric fields parallel to the [001] or [111] axis. Our estimates are in good agreement with the value measured by Feher, Shepherd, and Shore at 11°K. Agreement with the rate measured by Bron and Dreyfus at 1.4°K is obtained by allowing for an effective displacement of the dipole equilibrium position from a centrosymmetric position. The Raman transitions are shown to be strongly temperature-dependent, dominating the dipole-lattice relaxation processes at very low temperatures, while the direct transitions display a linear temperature dependence.

I. INTRODUCTION

In this paper we examine the phonon-induced relaxation of OH^- electric dipoles in low-temperature KCl crystals with a dc electric field applied parallel to either the [001] or [111] axis. Recent para-electric-resonance experiments by Feher, Shepherd, and Shore[1] have suggested that, for a 15.1 kV/cm dc electric field parallel to the [111] axis, this dipole-lattice relaxation rate is of order 10^{11} sec^{-1} at 11°K. Bron and Dreyfus[2] have estimated from the linewidth of the microwave resonance absorption in the presence of a weak [001] dc electric field that at 1.4°K the dipole-lattice relaxation rate is 3×10^8 sec^{-1}, a value which is in substantial agreement with the measurements of others.[3,4]

We use a point-charge–point-dipole model. The phonon electric field of the nearest-neighbor cluster is expanded in a power series in the local strains and their derivatives. The interaction of this field with the OH^- dipole is calculated. We also include the first-order terms arising from displacement of the dipole equilibrium position from the center of octahedral symmetry. That displacements of this kind can occur has been suggested by Bron and Dreyfus[2] for OH^-:KCl and Lombardo and Pohl[5] for Li-doped alkali halides. It is a well-known theorem of electrostatics that displacement of a point dipole is equivalent to superimposing a quadrupole moment on the dipole at its original position. The presence of the OH^- quadrupole moment can therefore be considered as equivalent to an effective dipole displacement. In our final estimate for the relaxation rate, we shall therefore be unable to distinguish between these two effects. We shall show that the measured relaxation rates in the low-temperature (helium) range can be accounted for only by allowing for such displacements. Our treatment will be limited to the direct and Raman terms of the phonon field because these terms dominate the relaxation at low temperatures.

Since OH^- is a light defect, the effect of the mass perturbation in the absence of changes in bonding will give rise to localized modes above the acoustic band.[6]

* Supported in part by the National Science Foundation and Office of Naval Research, Contract No. NONR 233(88).
† National Aeronautics and Space Administration Predoctoral Fellow.
[1] G. Feher, I. Shepherd, and H. Shore, Phys. Rev. Letters **16**, 500 (1966).
[2] W. Bron and R. Dreyfus, Phys. Rev. Letters **16**, 165 (1966).
[3] U. Kuhn and F. Luty, Solid State Commun. **4**, 31 (1965).
[4] U. Bosshard, R. Dreyfus, and W. Kanzig, Phys. Kondensierten Materie **4**, 254 (1965).
[5] G. Lombardo and R. Pohl, Phys. Rev. Letters **15**, 291 (1965).
[6] P. Dauber and R. Elliott, Proc. Roy. Soc. (London) **A273**, 222 (1963).

Since only the low-frequency acoustic phonons will be active in the direct processes and, for low temperatures, the dominant Raman phonons have frequencies well below the localized mode frequency, it is reasonable to assume that localized effects will not strongly affect the relaxation. If, however, there are strong bonding changes which give rise to low-lying localized modes, our results may be somewhat altered. We shall assume that the former case prevails and will use the unperturbed running-wave modes.

Kuhn and Luty[7] have demonstrated by optical methods that the OH^- dipoles in a field-free KCl crystal have equilibrium orientations along the [100] axes. Feher *et al.*,[1] and Shore[8] have described the behavior of the dipole eigenvalues and eigenfunctions when dc electric fields are applied parallel to the [001] or [111] axes. They choose as a basis the six states

$$|Z\rangle,\ |-Z\rangle,\ |Y\rangle,\ |-Y\rangle,\ |X\rangle,\ |-X\rangle,$$

and assume an overlap of states connected by $\frac{1}{2}\pi$ rotations in the presence of a strong octahedral crystalline field. This overlap yields nondiagonal matrix elements $-\frac{1}{2}\Delta$ for the field-free Hamiltonian and diagonalization produces a ground-state singlet A_{1g}, a triplet state T_{1u}, and a doublet state E_g, with the relative energies -2Δ, 0, Δ, respectively. In the high-field limit $E_0^2 p_u^2 \gg \Delta^2$ (where E_0 is the dc electric field and P_u is the dipole moment), the dipole levels split in the manner shown in Fig. 1. For rf electric fields parallel to the dc field (the arrangement used by Feher *et al.*,[1] and Bron and Dreyfus[2]) the first-order induced transitions are $1A_1 \rightarrow 2A_1$ and $2A_1 \rightarrow 3A_1$ in the presence of an [001] dc field and $1A_1 \rightarrow 2A_1$ and $1E \rightarrow 2E$ in the presence of a [111] dc field. These transitions are indicated by arrows in Fig. 1. It is the purpose of this paper to examine the relaxation of these four transitions.

II. PHONON ELECTRIC FIELD

We write the potential of an OH^- dipole, which has substituted for a Cl^- ion at the origin and has its equilibrium position displaced to $\mathbf{r}_e$, as

$$V(0)=\sum_{\mathbf{a}} \frac{e}{|\mathbf{a}+\mathbf{U}(\mathbf{a})-\mathbf{U}(0)-\mathbf{r}_e|}. \tag{1}$$

The $\mathbf{a}$'s are the lattice vectors of the six nearest-neighbor K^+ ions and $\mathbf{U}(\mathbf{a})$ and $\mathbf{U}(0)$ are the vibrational displacements of the K^+ and OH^- ions, respectively. This potential is expanded into a Taylor series in $\mathbf{U}_\alpha(\mathbf{a})-\mathbf{U}_\alpha(0)$ (α denotes the Cartesian axis) and the second-order expansion

$$U_\alpha(\mathbf{a})-U_\alpha(0)=\sum_\beta \epsilon_{\alpha\beta}(0)a_\beta+\tfrac{1}{2}\sum_{\beta,\gamma}\frac{\partial\epsilon_{\alpha\beta}(0)}{\partial r_\gamma}a_\beta a_\gamma \tag{2}$$

is introduced, where $\epsilon_{\alpha\beta}(0)$ is the $\alpha\beta$ component of the strain tensor at the origin,

$$\epsilon_{\alpha\beta}(0)=\frac{1}{2}\left[\frac{\partial U_\alpha(0)}{\partial r_\beta}+\frac{\partial U_\beta(0)}{\partial r_\alpha}\right]. \tag{3}$$

This latter expansion is valid only when $ka \ll 1$, where k is the phonon wave number and a is the nearest-neighbor distance. The result is next specialized to the O_h symmetry of the K^+ cluster surrounding the OH^- ion. The ratio of the noncentrosymmetric part of the phonon field (i.e., the part arising from the displacement $\mathbf{r}_e$) to the centrosymmetric part is of order r_e/ka^2 for a given phonon of wave number k. For the direct process, $ka \ll 1$, because the single phonon involved must be on "speaking terms" with the electric dipole transitions, i.e. the phonons must have the dipole transition energy. If the displacement ratio r_e/a is large compared to ka, the noncentrosymmetric field will dominate the direct dipole-lattice relaxation. For the Raman processes, however, the dominant phonons have wave numbers that are much larger than the dipole transition energy and ka will be large compared to r_e/a. Therefore the centrosymmetric part of the phonon field makes the dominant contribution to the Raman dipole-lattice relaxation and the noncentrosymmetric two-phonon term will be neglected. The relevant part of the phonon electric field at the dipole site is then found to be

$$E_\alpha=-\frac{e}{a}\Bigg\{2\frac{\partial\epsilon_{\alpha\alpha}(0)}{\partial r_\alpha}-\sum_{\beta\neq\alpha}\frac{\partial\epsilon_{\alpha\beta}(0)}{\partial r_\beta}+\frac{12}{a^2}\Big\{r_{e\alpha}\epsilon_{\alpha\alpha}(0)-\sum_{\beta\neq\alpha}\left[r_{e\beta}\epsilon_{\alpha\beta}(0)+\tfrac{1}{2}r_{e\alpha}\epsilon_{\beta\beta}(0)\right]\Big\}$$
$$-6\epsilon_{\alpha\alpha}(0)\frac{\partial\epsilon_{\alpha\alpha}(0)}{\partial r_\alpha}+3\sum_{\beta\neq\alpha}\left[\epsilon_{\alpha\beta}(0)\frac{\partial\epsilon_{\alpha\beta}(0)}{\partial r_\alpha}+\epsilon_{\alpha\beta}(0)\frac{\partial\epsilon_{\beta\beta}(0)}{\partial r_\beta}+\epsilon_{\beta\beta}(0)\frac{\partial\epsilon_{\alpha\beta}(0)}{\partial r_\beta}\right]\Bigg\}. \tag{4}$$

Note that the inversion symmetry about the octahedral site has allowed only derivatives of the strain to survive in the centrosymmetric one-phonon term and products of strains and their derivatives to survive in the centrosymmetric two-phonon term. The lowering of the symmetry that results from the displacement $\mathbf{r}_e$, however,

[7] U. Kuhn and F. Luty, Solid State Commun. 2, 281 (1964).
[8] H. B. Shore, Phys. Rev. 151, 570 (1966).

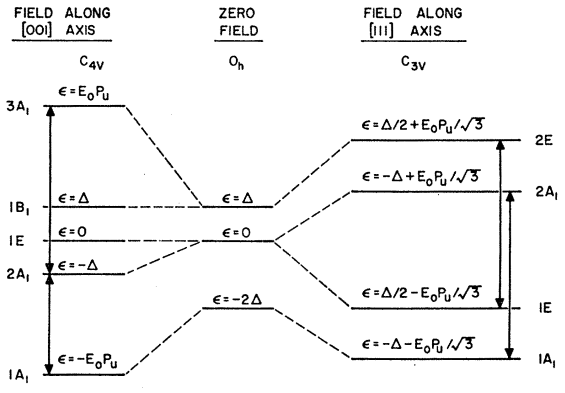

FIG. 1. Eigenvalues of OH^- dipoles in KCl for $E_0^2P_u^2\gg\Delta^2$. From H. B. Shore, Phys. Rev. **151**, 570 (1966).

has allowed strains to appear in the noncentrosymmetric one-phonon term.[9]

III. TRANSITION AMPLITUDES

The Raman relaxation will arise from two mechanisms —the two-phonon electric field inducing first-order dipole transitions (using the first-order transition amplitude), and the one-phonon electric field inducing second-order dipole transitions (using the second-order transition amplitude). The two-phonon electric field differs from the one-phonon field by a factor of the order of a strain. Thus, approximating the dipole-moment matrix elements by P_u, the ratio of the second-order transition amplitude to the first-order amplitude for Raman transitions is of order $ekP_u/a\hbar\omega$ for a given phonon of wave number k and frequency ω. For KCl this ratio is $\sim 4\times 10^2$. Thus we conclude that if the dipole-moment matrix elements in the second-order transition amplitude are not too small, and do not cancel each other, the second-order amplitude will yield the dominant Raman relaxation rate.

The transition matrix elements of the dipole-moment operator are tabulated in Tables I and II. We introduce the well-known expression for the normal-mode acoustic vibrations of a monatomic lattice (neglecting the effects of the 9% mass difference of K and Cl) into Eq. (4), using the defining equation (3). We then use the dipole-moment matrix elements of Tables I and II and the phonon creation- and destruction-operator matrix elements to compute the transition amplitudes of the dipole-phonon system. For the purpose of averaging the squared transition amplitudes over the phonon energy surfaces in reciprocal space we assume that the dispersion is sufficiently isotropic to allow us to approximate the energy surfaces by spheres. Accepting this assumption it is a corollary that the transverse polarization eigenvector is perpendicular to the wave vector for all directions. We use Euler angles to describe the polarization and wave vectors and use the following averages for transverse phonons:

$$
\begin{aligned}
[\mu_\alpha^2(\mathbf{k},j)k_\alpha^2]_{\rm av}&=k^2/15\\
[\mu_\alpha^2(\mathbf{k},j)k_\beta^2]_{\rm av}&=2k^2/15 \quad (\alpha\neq\beta)\\
[\mu_\alpha(\mathbf{k},j)\mu_\beta(\mathbf{k},j)k_\alpha k_\beta]_{\rm av}&=-k^2/30 \quad (\alpha\neq\beta)\\
[\mu_\alpha^2(\mathbf{k},j)k_\beta k_\gamma]_{\rm av}&=0 \quad (\beta\neq\gamma)\\
[\mu_\alpha(\mathbf{k},j)\mu_\beta(\mathbf{k},j)k_\alpha^2]_{\rm av}&=0 \quad (\alpha\neq\beta)\\
[\mu_\alpha(\mathbf{k},j)\mu_\beta(\mathbf{k},j)k_\gamma k_\sigma]_{\rm av}&=0 \quad (\alpha\neq\beta,\ \beta\neq\gamma,\ \gamma\neq\alpha)\\
[\mu_\alpha^2(\mathbf{k},j)k_\alpha^4]_{\rm av}&=k^2/35\\
[\mu_\alpha^2(\mathbf{k},j)k_\beta^4]_{\rm av}&=3k^2/35 \quad (\alpha\neq\beta)\\
[\mu_\alpha^2(\mathbf{k},j)k_\alpha^2k_\beta^2]_{\rm av}&=2k^2/105 \quad (\alpha\neq\beta)\\
[\mu_\alpha^2(\mathbf{k},j)k_\beta^2k_\gamma^2]_{\rm av}&=k^2/35 \quad (\alpha\neq\beta,\ \beta\neq\gamma,\ \gamma\neq\alpha)\\
[\mu_\alpha(\mathbf{k},j)\mu_\beta(\mathbf{k},j)k_\gamma^2k_\sigma^2]_{\rm av}&=0 \quad (\alpha\neq\beta),
\end{aligned}
\tag{5}
$$

where $\mathbf{u}(\mathbf{k},j)$ is the unit polarization eigenvector for a phonon of wave vector $\mathbf{k}$ and branch j. We omit

TABLE I. Transition matrix elements of the dipole-moment operator for [001] dc electric fields.

Matrix element	Weak field ($E_0^2P_u^2\ll\Delta^2$)	Strong field ($E_0^2P_u^2\gg\Delta^2$)
$\langle 3A_1\vert\mathbf{P}_{\rm op}\vert 1B_1\rangle$	0	0
$\langle 3A_1\vert\mathbf{P}_{\rm op}\vert 1E\rangle$	$-(P_u/\sqrt{6})(\hat{X}+\hat{Y})$	$-(1/\sqrt{2})(\Delta/E_0)(\hat{X}+\hat{Y})$
$\langle 3A_1\vert\mathbf{P}_{\rm op}\vert 2A_1\rangle$	$(2P_u/\sqrt{6})\hat{Z}$	$(\Delta/E_0)\hat{Z}$
$\langle 3A_1\vert\mathbf{P}_{\rm op}\vert 1A_1\rangle$	0	0
$\langle 1B_1\vert\mathbf{P}_{\rm op}\vert 1E\rangle$	$(P_u/\sqrt{2})(\hat{X}-\hat{Y})$	$(P_u/\sqrt{2})(\hat{X}-\hat{Y})$
$\langle 1B_1\vert\mathbf{P}_{\rm op}\vert 2A_1\rangle$	0	0
$\langle 1B_1\vert\mathbf{P}_{\rm op}\vert 1A_1\rangle$	0	0
$\langle 1E\vert\mathbf{P}_{\rm op}\vert 2A_1\rangle$	$-\frac{1}{2}(E_0/\Delta)P_u^2(\hat{X}+\hat{Y})$	$-(P_u/\sqrt{2})(\hat{X}+\hat{Y})$
$\langle 1E\vert\mathbf{P}_{\rm op}\vert 1A_1\rangle$	$(P_u/\sqrt{3})(\hat{X}+\hat{Y})$	$(1/\sqrt{2})(\Delta/E_0)(\hat{X}+\hat{Y})$
$\langle 2A_1\vert\mathbf{P}_{\rm op}\vert 1A_1\rangle$	$(P_u/\sqrt{3})\hat{Z}$	$(\Delta/E_0)\hat{Z}$

TABLE II. Transition matrix elements of the dipole-moment operator for [111] dc electric fields. $\hat{l}_1=(1/\sqrt{6})(2\hat{Z}-\hat{X}-\hat{Y})$, $\hat{l}_2=(1/\sqrt{2})(\hat{X}-\hat{Y})$, $\hat{l}_3=(1/\sqrt{3})(\hat{X}+\hat{Y}+\hat{Z})$.

Matrix element	Weak field ($E_0^2P_u^2\ll\Delta^2$)	Strong field ($E_0^2P_u^2\gg\Delta^2$)
$\langle 2E\vert\mathbf{P}_{\rm op}\vert 2A_1\rangle$	$(P_u/\sqrt{3})(\hat{l}_1+\hat{l}_2)$	$-(P\pi/\sqrt{3})(\hat{l}_1+\hat{l}_2)$
$\langle 2E\vert\mathbf{P}_{\rm op}\vert 1E\rangle$	$\frac{2P_u}{\sqrt{6}}(2\sqrt{2}\hat{l}_3-\hat{l}_1-\hat{l}_2)$	$\frac{1}{\sqrt{2}}\frac{\Delta}{E_0}(2\sqrt{2}\hat{l}_3-\hat{l}_1-\hat{l}_2)$
$\langle 2E\vert\mathbf{P}_{\rm op}\vert 1A_1\rangle$	$-\frac{1}{6}(E_0/\Delta)P_u^2(\hat{l}_1+\hat{l}_2)$	$-\frac{1}{4}(\Delta/E_0)(\hat{l}_1+\hat{l}_2)$
$\langle 2A_1\vert\mathbf{P}_{\rm op}\vert 1E\rangle$	$\frac{1}{6}(E_0/\Delta)P_u^2(\hat{l}_1+\hat{l}_2)$	$-\frac{1}{4}(\Delta/E_0)(\hat{l}_1+\hat{l}_2)$
$\langle 2A_1\vert\mathbf{P}_{\rm op}\vert 1A_1\rangle$	$(P_u/\sqrt{3})\hat{l}_3$	$-(\Delta/E_0)\hat{l}_3$
$\langle 1E\vert\mathbf{P}_{\rm op}\vert 1A_1\rangle$	$(P_u/\sqrt{3})(\hat{l}_1+\hat{l}_2)$	$(P_u/\sqrt{3})(\hat{l}_1+\hat{l}_2)$

[9] It is helpful to draw a comparison between the dipole-lattice and spin-lattice interactions. In the latter case, the paramagnetic electron interacts with the phonon electric potential, while in the former case it is the phonon electric field (gradient of the phonon electric potential with respect to the dipole position r_e) that couples the dipole to the lattice. The electron phonon potential is obtained by integrating E_α with respect to $r_{e\alpha}$ and identifying r_e with the electronic coordinate. We thus see from (4) that the electron-phonon term active in direct spin-lattice relaxation will depend on the local strains, not their derivatives. For a complete discussion of the spin-lattice mechanism one may refer to J. Van Vleck's paper [Phys. Rev. **57**, 426 (1940)].

consideration of longitudinal phonons because, as will become clear later, the transverse phonons strongly dominate the relaxation processes.

IV. TRANSITION RATES

Karo[10] has calculated the density of states of the acoustic modes in KCl. His results display a close agreement with the Debye density of states up to $\omega\sim 1.5\times 10^{13}$ sec^{-1}, well above the energy of the phonons which contribute to both the direct and Raman relaxation processes when the temperature is low. Hence we use the density of states

$$\rho_j = Vk^2/2\pi^2 v_j \tag{6}$$

for the jth branch, where v_j is the corresponding velocity of sound and V is the crystal volume. For the direct processes we may use the first-order approximation $k=\omega(k,j)/v_j$ because of the small energy of the interacting phonon. For the Raman processes, however, the dominant phonons lie too far out in the zone for temperatures greater than $\sim 5°$ K to use a nondispersive spectrum with sufficient validity, and we shall have to include the effects of dispersion.

Inserting the angular averages of the first- and second-order squared transition amplitudes into Fermi's golden rule we find the transition rates per dipole between the initial dipole state ϕ_i and final state ϕ_f with energies ϵ_i and ϵ_f, respectively. The centrosymmetric *direct* transition rate is

$$W_{i\to f}=\frac{3\times 10^{-2}e^2}{a^2\rho\hbar^6}\left[\frac{\exp([\epsilon_i-\epsilon_f]/kT)+1}{\exp([\epsilon_i-\epsilon_f]/kT)-1}\right]\times\sum_\alpha|\langle\phi_f|P_{\mathrm{op}}{}^\alpha|\phi_i\rangle|^2\sum_j\frac{(\epsilon_i-\epsilon_f)^5}{v_j{}^7}, \tag{7}$$

and the noncentrosymmetric *direct* transition rate is

$$W_{i\to f}=\frac{23e^2}{a^4\rho\hbar^4}\left[\frac{\exp([\epsilon_i-\epsilon_f]/kT)+1}{\exp([\epsilon_i-\epsilon_f]/kT)-1}\right]\times\sum_\alpha\left[\left(0.15\frac{r_{e\alpha}{}^2}{a^2}+0.27\sum_{\beta\neq\alpha}\frac{r_{e\beta}{}^2}{a^2}\right)|\langle\phi_f|P_{\mathrm{op}}{}^\alpha|\phi_i\rangle|^2-\sum_{\beta\neq\alpha}0.11\frac{r_{e\alpha}r_{e\beta}}{a^2}|\langle\phi_f|P_{\mathrm{op}}{}^\alpha|\phi_i\rangle||\langle\phi_f|P_{\mathrm{op}}{}^\beta|\phi_i\rangle|\right]\times\sum_j\frac{(\epsilon_i-\epsilon_f)^3}{v_j{}^5} \tag{8}$$

where ρ is the crystal density. The *Raman* rate for the second-order phonon field is

$$W_{i\to f}=\frac{10^{-2}e^2}{a^2\rho^2}\left[1+\exp\left(-\frac{\epsilon_i-\epsilon_f}{kT}\right)\right]\sum_\alpha|\langle\phi_f|P_{\mathrm{op}}{}^\alpha|\phi_i\rangle|^2\times\sum_j\frac{1}{v_j}\int\frac{k^{10}\exp[\hbar\omega(k,j)/kT]dk}{\omega(k,j)^2\{\exp[\hbar\omega(k,j)/kT]-1\}^2}, \tag{9}$$

and the *Raman* rate for second-order dipole transitions is

$$W_{i\to f}=\frac{6.5\times 10^{-4}e^4}{a^4\rho^2\hbar^2}[1+\exp(-[\epsilon_i-\epsilon_f]/kT)]\times\sum_{\alpha,\beta}|\sum_n\langle\phi_f|P_{\mathrm{op}}{}^\alpha|\phi_n\rangle\langle\phi_n|P_{\mathrm{op}}{}^\beta|\phi_i\rangle|^2\times\sum_j\frac{1}{v_j}\int\frac{k^{12}\exp[\hbar\omega(k,j)/kT]dk}{\omega(k,j)^4\{\exp[\hbar\omega(k,j)/kT]-1\}^2}. \tag{10}$$

We see that all four transition rates are strongly dominated by the lowest branch of the acoustic spectrum. If a nondispersive spectrum were assumed for the Raman rates the transition rates (7) through (10) would be proportional to v_j^{-7}, v_j^{-5}, v_j^{-12}, and v_j^{-14}, respectively, so that our earlier assertion that the transverse modes dominate the relaxation is verified. Tenerz[11] has calculated a frequency spectrum of KCl that is in excellent agreement with sound-velocity data. Parallel to the [001] axes his transverse-acoustic spectrum can be fitted by a sine-type dispersion,

$$\omega(k,t)=1.08\times 10^{13}\sin\tfrac{1}{2}ka, \tag{11}$$

which coincides with the long-wave region but is $\sim 10\%$ greater at the zone boundary. Since the transverse-acoustic velocities are lowest along the [100] axes we assume that the dominant dispersion is displayed by Eq. (11). Feher *et al.*[1] have measured the effective dipole moment P_u and zero-field splitting Δ. They find

$$P_u=4\times 10^{-18}\text{ esu}\qquad \Delta=6.2\times 10^9\text{ cps }(0.30°\text{K}). \tag{12}$$

We use Eqs. (11) and (12) and the constants of the KCl lattice to estimate the magnitudes of the rates (7) through (10) for the dipole-lattice relaxations of interest to us here. The results are tabulated in Tables III–VI.

The direct rates display the well-known linear temperature dependence for $T>1$°K. It is of interest to note that the two Raman rates would display a T^9 temperature dependence in the absence of dispersion, rather than the T^7 dependence normally found in the absence of Kramers degeneracy. The extra two powers of T have arisen from the fact that both the one- and two-phonon centrosymmetric fields in Eq. (4) contain a derivative of the strain. When these two fields enter into the expressions for the two Raman transition rates this derivative introduces two extra powers of k so that two extra powers of T appear in the nondispersive case. For the same reason the direct centrosymmetric transition rate displays a fifth-power dependence on the phonon energy rather than the third-power dependence that is normally expected (the third-power dependence does appear in the direct noncentrosymmetric rate because of its dependence on lattice strains instead of their derivatives). These conclusions are valid for any

[10] A. Karo, J. Chem. Phys. 33, 7 (1960).

[11] E. Tenerz, Arkiv Fysik 12, 281 (1957).

TABLE III. Dipole-lattice relaxation rates for a strong [001] dc electric field ($E_0^2P_u^2 \gg \Delta^2$).

Transition	
	Direct centrosymmetric rate
$2A_1 \rightarrow 1A_1$ $3A_1 \rightarrow 2A_1$	$W=3.5\left[\dfrac{\exp(0.03[E_0/T])+1}{\exp(0.03[E_0/T])-1}\right]E_0^3$
	Direct noncentrosymmetric rate
$2A_1 \rightarrow 1A_1$ $3A_1 \rightarrow 2A_1$	$W=3.1\times10^8\left[\dfrac{\exp(0.03[E_0/T])+1}{\exp(0.03[E_0/T])-1}\right]\left[\dfrac{r_{ez}^2}{a^2}+1.8\dfrac{r_{ez}^2+r_{ey}^2}{a^2}\right]E_0$
	Raman rate for second-order phonon field
$2A_1 \rightarrow 1A_1$ $3A_1 \rightarrow 2A_1$	$W=3.5\times10^{12}[\exp(-0.03\{E_0/T\})+1]E_0^{-2}\displaystyle\int_{u=0}^{u=\pi}\frac{u^{10}\exp([78/T]\sin[u/2])du}{\sin^2(u/2)[\exp(\{78/T\}\sin\{u/2\})-1]^2}$
	Raman rate for second-order dipole transitions
$2A_1 \rightarrow 1A_1$ $3A_1 \rightarrow 2A_1$	$W=3.7\times10^{15}[\exp(-0.03\{E_0/T\})+1]E_0^{-2}\displaystyle\int_{u=0}^{u=\pi}\frac{u^{12}\exp([78/T]\sin[u/2])du}{\sin^4(u/2)[\exp(\{78/T\}\sin\{u/2\})-1]^2}$

TABLE IV. Dipole-lattice relaxation rates for a weak [001] dc electric field ($E_0^2P_u^2 \ll \Delta^2$).

Transition	
	Direct centrosymmetric rate
$2A_1 \rightarrow 1A_1$	$W=2.8\times10^4\left[\dfrac{\exp(0.6/T)+1}{\exp(0.6/T)-1}\right]$
$3A_1 \rightarrow 2A_1$	$W=1.7\times10^3\left[\dfrac{\exp(0.3/T)+1}{\exp(0.3/T)-1}\right]$
	Direct noncentrosymmetric rate
$2A_1 \rightarrow 1A_1$	$W=8.0\times10^9\left[\dfrac{\exp(0.6/T)+1}{\exp(0.6/T)-1}\right]\left[\dfrac{r_{ez}^2}{a^2}+1.8\dfrac{r_{ez}^2+r_{ey}^2}{a^2}\right]$
$3A_1 \rightarrow 2A_1$	$W=2.0\times10^9\left[\dfrac{\exp(0.3/T)+1}{\exp(0.3/T)-1}\right]\left[\dfrac{r_{ez}^2}{a^2}+1.8\dfrac{r_{ez}^2+r_{ey}^2}{a^2}\right]$
	Raman rate for second-order phonon field
$2A_1 \rightarrow 1A_1$	$W=1.1\times10^{10}[\exp(-0.6/T)+1]\displaystyle\int_{u=0}^{u=\pi}\frac{u^{10}\exp([78/T]\sin[u/2])du}{\sin^2(u/2)[\exp(\{78/T\}\sin\{u/2\})-1]^2}$
$3A_1 \rightarrow 2A_1$	$W=2.2\times10^{10}[\exp(-0.3/T)+1]\displaystyle\int_{u=0}^{u=\pi}\frac{u^{10}\exp([78/T]\sin[u/2])du}{\sin^2(u/2)[\exp(\{78/T\}\sin\{u/2\})-1]^2}$
	Raman rate for second-order dipole transitions
$2A_1 \rightarrow 1A_1$	$W=1.1\times10^{11}[\exp(-0.6/T)+1]E_0^2\displaystyle\int_{u=0}^{u=\pi}\frac{u^{12}\exp([78/T]\sin[u/2])du}{\sin^4(u/2)[\exp(\{78/T\}\sin\{u/2\})-1]^2}$
$3A_1 \rightarrow 2A_1$	$W=5.5\times10^{10}[\exp(-0.3/T)+1]E_0^2\displaystyle\int_{u=0}^{u=\pi}\frac{u^{12}\exp([78/T]\sin[u/2])du}{\sin^4(u/2)[\exp(\{78/T\}\sin\{u/2\})-1]^2}$

lattice possessing inversion symmetry about the (undisplaced) dipole site.

Note that the Raman processes via the second-order dipole transitions vanish for a dc field parallel to the [111] axis, due to cancellation between the intermediate states in Eq. (10). This cancellation does not occur, however, for an [001] dc field. For sufficiently large dc fields ($E_0 \gtrsim 300$ V/cm) this will result in a faster Raman relaxation rate with the field parallel to the [001] axis than with the field parallel to the [111] axis.

V. COMPARISON WITH EXPERIMENT

The integrals appearing in the Raman rates of Tables III–IV have been evaluated numerically. For a 15.1-kV/cm (50 esu) dc electric field parallel to the [111] axis, the direct centrosymmetric and Raman dipole-

TABLE V. Dipole-lattice relaxation rates for a strong [111] dc electric field ($E_0^2P_u^2 \gg \Delta^2$).

Transition	
	Direct centrosymmetric rate
$2E \rightarrow 1E$ $2A_1 \rightarrow 1A_1$	$W=7.0\left[\dfrac{\exp(0.03[E_0/T])+1}{\exp(0.03[E_0/T])-1}\right]E_0^3$
	Direct noncentrosymmetric rate
$2E \rightarrow 1E$	$W=7.0\times10^8\left[\dfrac{\exp(0.03[E_0/T])+1}{\exp(0.03[E_0/T])-1}\right]\left[\dfrac{r_e^2}{a^2}-0.08\dfrac{r_{ez}r_{ex}+r_{ez}r_{ey}+r_{ex}r_{ey}}{a^2}\right]E_0$
$2A_1 \rightarrow 1A_1$	$W=7.0\times10^8\left[\dfrac{\exp(0.03[E_0/T])+1}{\exp(0.03[E_0/T])-1}\right]\left[\dfrac{r_e^2}{a^2}-0.32\dfrac{r_{ez}r_{ex}+r_{ez}r_{ey}+r_{ex}r_{ey}}{a^2}\right]E_0$
	Raman rate for second-order phonon field
$2E \rightarrow 1E$ $2A_1 \rightarrow 1A_1$	$W=3.5\times10^{12}[\exp(-0.03\{E_0/T\})+1]E_0^{-2}\displaystyle\int_{u=0}^{u=\pi}\frac{u^{10}\exp([78/T]\sin[u/2])du}{\sin^2(u/2)[\exp(\{78/T\}\sin\{u/2\})-1]^2}$
	Raman rate for second-order dipole transitions
$2E \rightarrow 1E$ $2A_1 \rightarrow 1A_1$	$W=0$

TABLE VI. Dipole-lattice relaxation rates for a weak [111] dc electric field ($E_0^2P_u^2 \ll \Delta^2$).

Transition	
	Direct centrosymmetric rate
$2E \rightarrow 1E$	$W=3.5\times10^3\left[\dfrac{\exp(0.3/T)+1}{\exp(0.3/T)-1}\right]$
$2A_1 \rightarrow 1A_1$	$W=2.8\times10^4\left[\dfrac{\exp(0.6/T)+1}{\exp(0.6/T)-1}\right]$
	Direct noncentrosymmetric rate
$2E \rightarrow 1E$	$W=6.5\times10^9\left[\dfrac{\exp(0.3/T)+1}{\exp(0.3/T)-1}\right]\left[\dfrac{r_e^2}{a^2}-0.31\dfrac{r_{ez}r_{ex}+r_{ez}r_{ey}+r_{ex}r_{ey}}{a^2}\right]$
$2A_1 \rightarrow 1A_1$	$W=1.3\times10^{10}\left[\dfrac{\exp(0.6/T)+1}{\exp(0.6/T)-1}\right]\left[\dfrac{r_e^2}{a^2}-0.31\dfrac{r_{ez}r_{ex}+r_{ez}r_{ey}+r_{ex}r_{ey}}{a^2}\right]$
	Raman rate for second-order phonon field
$2E \rightarrow 1E$	$W=4.4\times10^{10}[\exp(-0.3/T)+1]\displaystyle\int_{u=0}^{u=\pi}\frac{u^{10}\exp([78/T]\sin[u/2])du}{\sin^2(u/2)[\exp(\{78/T\}\sin\{u/2\})-1]^2}$
$2A_1 \rightarrow 1A_1$	$W=1.1\times10^{10}[\exp(-0.6/T)+1]\displaystyle\int_{u=0}^{u=\pi}\frac{u^{10}\exp([78/T]\sin[u/2])du}{\sin^2(u/2)[\exp(\{78/T\}\sin\{u/2\})-1]^2}$
	Raman rate for second-order dipole transitions
$2E \rightarrow 1E$ $2A_1 \rightarrow 1A_1$	$W=0$

lattice relaxation rates (Table V) for temperatures in the range 2° to 11°K are plotted in Fig. 2. The Raman rate is larger than the centrosymmetric direct rate for temperatures greater than ~4°K and at 11°K the Raman rate is 7.1×10^{10} sec^{-1}, in good agreement with the observations of Feher *et al.*[1] If a nondispersive spectrum were assumed, the resulting Raman rate at 11°K would be 10^9 sec^{-1}, two orders of magnitude smaller than that found in the presence of dispersion. Thus, the decrease in slope of the transverse-acoustic branches at the higher frequencies has an enormous effect on the Raman relaxation rate.

In the above computation we have omitted a numerical estimate of the noncentrosymmetric direct rate

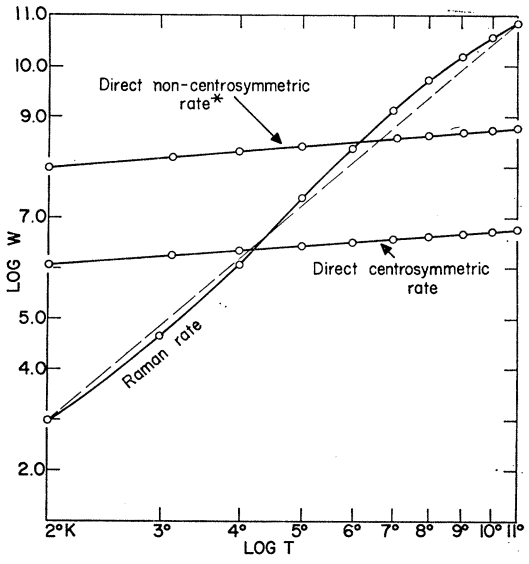

FIG. 2. A plot of the log of the dipole-lattice relaxation rate versus the log of the temperature for a 15.1 kV/cm dc electric field parallel to the [111] axis. The dotted line represents a T^{11} temperature dependence. (*) The noncentrosymmetric rate is for the noncentrosymmetric dipole position determined from the data of Bron and Dreyfus at 1.4°K.

because of lack of knowledge of the displacement of the dipole equilibrium position from the center of octahedral symmetry. A comparison of this rate with the centrosymmetric direct rate in Table V reveals that the noncentrosymmetric direct rate will be dominant for a displacement ratio $r_e/a > 5\times10^{-3}$ when a 15.1 kV/cm dc field is applied parallel to the [111] axis. One way of estimating the magnitude of r_e is by comparing our expression for the direct relaxation rates with the rates that have been measured at low temperatures,[2-4] where the direct processes dominate. The direct centrosymmetric relaxation rate for a weak [001] dc field at 1.4°K is 1.7×10^4 sec^{-1}, four orders of magnitude below the experimental values. If we allow a displacement $r_e\sim0.3$ Å of the dipole equilibrium position from the centrosymmetric site, however, the noncentrosymmetric direct relaxation rate will be 3×10^8 sec^{-1}, in agreement with that measured by Bron and Dreyfus.[2] It is interesting to note that if we assume a somewhat crude model of the dipole where the oxygen and hydrogen ions are separated by an amount necessary to give the dipole moment measured by Feher *et al.*,[1] then the effective dipole "displacement" arising from the quadrupole moment of the two ions turns out to be 0.4 Å. This suggests that the quadrupole relaxation rate is of the same order as that given by real displacements of the dipole equilibrium position. As soon as reliable values for the OH^- quadripole moment are known these two effects can be separated from one another. At the present time in any case, we have shown that reasonable estimates for the displacement of the OH^- ion are capable of explaining the entirety of the low-temperature relaxation behavior.

We use this fitted value of the displacement to plot the noncentrosymmetric relaxation rate, for a 15.1-kV/cm dc field parallel to the [111] axis, in Fig. 2. This direct dipole-lattice relaxation rate is intersected by the Raman rate at 6°K.

VI. CONCLUSION

Agreement between the experimental and theoretical dipole-lattice relaxation rates has been obtained in the direct process region by allowing for an effective displacement of the dipole equilibrium position from the center of octahedral symmetry. This displacement does not have a first-order effect on the Raman processes and a centrosymmetric model appears to fit the Raman data rather well. The Raman relaxation displays a strong temperature dependence, increasing as T^9 for the nondispersive case, and increasing even faster with temperature when dispersion is introduced (see Fig. 2). The effects of dispersion strongly affect the Raman relaxation, enhancing it by two orders of magnitude at 11°K. The direct relaxation rate displays a linear temperature dependence and is overtaken by the Raman relaxation rate at very low temperatures. For sufficiently large dc electric fields ($E_0\gtrsim300$ V/cm) the Raman relaxation rate with the field parallel to the [001] axis will be greater than the rate with the field parallel to the [111] axis.

It should be noted that at temperatures greater than ~5°K the long-wave approximation which is implicit in Eq. (2) becomes suspect for Raman processes. For these higher temperatures one should include higher order terms in the expansion (2). Our theory, however, does fit the experimental data rather well at temperatures as high as 11°K.

ACKNOWLEDGMENTS

The author wishes to express his appreciation to Professor Raymond L. Orbach who suggested this work and made many helpful suggestions, and to Professor G. Feher and Dr. Herbert Shore for helpful discussion.